

Table 2. Nonrelativistic Hartree–Fock and relativistic Dirac–Hartree–Fock orbital eigenvalues ( $\epsilon$ ) and radial expectation values ( $\langle r \rangle$ ) for the ns and np orbitals of Rn and (118).

Element Rn			Element 118		
Orbital	$\epsilon$ [eV]	$\langle r \rangle$ [Å]	Orbital	$\epsilon$ [eV]	$\langle r \rangle$ [Å]
nonrelativistic			nonrelativistic		
6s	–23.78	1.14	7s	–21.06	1.28
6p	–11.65	1.35	7p	–10.73	1.49
relativistic			relativistic		
6s <sub>1/2</sub>	–29.19	1.02	7s <sub>1/2</sub>	–36.25	0.96
6p <sub>1/2</sub>	–14.71	1.19	7p <sub>1/2</sub>	–20.29	1.09
6p <sub>3/2</sub>	–10.45	1.37	7p <sub>3/2</sub>	–8.25	1.58

7p<sub>1/2</sub> spinors are stabilized by 12 eV and radially contracted by 0.5 Å relative to the 7p<sub>3/2</sub> spinors. As is evident in Table 2, these effects are much greater in (118) than for the corresponding orbitals in Rn. The large relative stabilization and radial contraction of the 7s<sub>1/2</sub> and 7p<sub>1/2</sub> spinors of (118) essentially make them unavailable for bonding interactions with the F atoms. Thus, the four electrons that can be described by these spinors are rendered as stereochemically inactive “inert pairs”.<sup>[9c]</sup> From the point of view of the VSEPR model, the number of electron-pair domains has been reduced from six to four, consistent with a tetrahedral geometry within that model. The generation of inert pairs in conjunction with the expected large radius of (118) are consistent with our prediction that the tetrahedral and square-planar forms of (118)F<sub>4</sub> are practically isoenergetic, a remarkable consequence of large spin-orbit coupling.

Received: July 20, 1998 [Z12183IE]

German version: *Angew. Chem.* **1999**, *111*, 115–117

**Keywords:** electronic structure • noble gases • spin-orbit coupling • transuranium elements • VSEPR model

- [1] a) S. Hofmann, V. Ninov, F. P. Hessberger, P. Armbruster, H. Folger, G. Muenzenberg, H. J. Schoett, A. G. Popeko, A. V. Yerebin, *Z. Phys. A* **1996**, *354*, 229; b) P. Armbruster, *Bull. Soc. Fr. Phys.* **1996**, *107*, 6.
- [2] Examples: a) V. Pershina, *Chem. Rev.* **1996**, *96*, 1977; b) M. Jacoby, *Chem. Eng. News* **1998**, *76*(12), 48–54.
- [3] Nomenclature: For unnamed elements, the atomic symbol is represented as (atomic number), such as (118).
- [4] *Noble-Gas Compounds* (Ed.: H. H. Hyman), University of Chicago Press, Chicago, **1963**.
- [5] R. J. Gillespie, R. S. Nyholm, *Q. Rev. Chem. Soc.* **1957**, 339.
- [6] R. J. Gillespie, *Angew. Chem.* **1996**, *108*, 539; *Angew. Chem. Int. Ed. Engl.* **1996**, *35*, 495.
- [7] P. Laszlo, G. J. Schrobilgen, *Angew. Chem.* **1988**, *100*, 495; *Angew. Chem. Int. Ed. Engl.* **1988**, *27*, 479.
- [8] a) V. V. Avrorin, R. N. Krasikova, V. D. Nefedov, M. A. Toropova, *Radiokhimiya* **1981**, *23*, 879; b) L. Stein, *Inorg. Chem.* **1984**, *23*, 3670.
- [9] Reviews of relativistic effects: a) K. S. Pitzer, *Acc. Chem. Res.* **1979**, *12*, 271; b) P. Pyykkö, J.-P. Desclaux, *Acc. Chem. Res.* **1979**, *12*, 276; c) P. Pyykkö, *Chem. Rev.* **1988**, *88*, 563; d) W. C. Ermler, R. B. Ross, P. A. Christiansen, *Adv. Quantum Chem.* **1988**, *19*, 139; e) M. Pepper, B. E. Bursten, *Chem. Rev.* **1991**, *91*, 719; f) K. Balasubramanian, *Relativistic Effects in Chemistry, Part A: Theory and Techniques*, Wiley, New York, **1997**.
- [10] E. Eliav, U. Kaldor, Y. Ishikawa, P. Pyykkö, *Phys. Rev. Lett.* **1996**, *77*, 5350.
- [11] C. S. Nash, B. E. Bursten, unpublished results.

- [12] Computational details: RCI calculations were carried out using Pitzer's modification of the COLUMBUS quantum-chemistry suite to allow inclusion of a spin-orbit potential.<sup>[13]</sup> Core electrons were replaced with shape-consistent relativistic effective core potentials (RECPs), which include spin-orbit operators.<sup>[14]</sup> The valence basis set consisted of (6p6sd1f) Gaussians contracted to [5p5sd1f]. The active space in the spin-orbit CI calculations consisted of single excitations of 24 electrons in 12 doubly occupied molecular orbitals into 14 virtual orbitals. Selected double excitations were also included in the active set. A typical calculation involved 3876 configurations and 24657 determinants under  $T_d$  symmetry and 1548 configurations and 9633 determinants under  $D_{4h}$ . Complete computational details will be given elsewhere.<sup>[11]</sup>
- [13] a) R. Shepard, I. Shavitt, R. M. Pitzer, D. C. Comeau, M. Pepper, H. Lischka, P. G. Szalay, R. Ahlrichs, F. B. Brown, J. G. Zhao, *Int. J. Quantum Chem. Symp.* **1989**, *22*, 149; b) A. Chang, R. M. Pitzer, *J. Am. Chem. Soc.* **1989**, *111*, 2500.
- [14] a) R. B. Ross, J. M. Powers, T. Atashroo, W. C. Ermler, L. A. LaJohn, P. A. Christiansen, *J. Chem. Phys.* **1990**, *93*, 6654, **1994**, *101*, 10198; b) C. S. Nash, B. E. Bursten, W. C. Ermler, *J. Chem. Phys.* **1997**, *106*, 5133.
- [15] a) J. Styszynski, G. L. Malli, *Int. J. Quantum Chem.* **1995**, *55*, 227; b) J. Styszynski, X. Cao, G. L. Malli, L. Visscher, *J. Comput. Chem.* **1997**, *18*, 601.
- [16] H. Bürger, S. Ma, J. Breidung, W. Thiel, *J. Chem. Phys.* **1996**, *104*, 4945.
- [17] J. H. Burns, P. A. Agron, H. A. Levy, *Science* **1963**, *139*, 1208.
- [18] M. Dolg, W. Kuchle, H. Stoll, H. Preuss, P. Schwerdtfeger, *Mol. Phys.* **1991**, *74*, 1265.
- [19] J. P. Desclaux, *At. Data Nucl. Data Tables* **1973**, *12*, 311.

## A New Type of Metal–Organic Large-Pore Zeotype\*\*

David M. L. Goodgame,\* David A. Grachvogel, and David J. Williams\*

The great industrial importance of zeolites, particularly in the petrochemicals industry, has fuelled the continuing interest in the synthesis and applications of new types of zeolites and related microporous materials (zeotypes). Particularly attractive avenues of further exploration include the incorporation of redox-active metals into such frameworks to provide novel heterogeneous catalytic systems<sup>[1]</sup> and the formation of zeotypes comprising microporous metal-organic ligand coordination arrays.<sup>[2]</sup> The latter approach offers, in principle, an extensive capability of custom-designing frameworks to gain better control of the pore sizes and shapes, whilst also permitting the incorporation of a wide range of metal ions, either as part of the framework or in the form of an

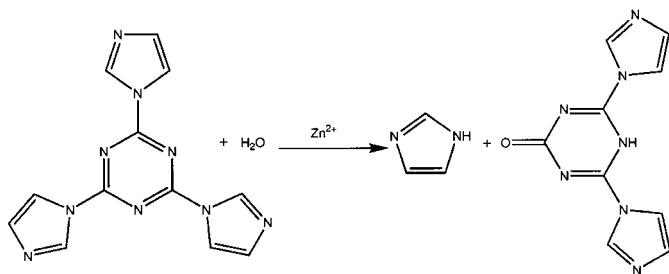
[\*] Prof. D. M. L. Goodgame, Prof. D. J. Williams, D. A. Grachvogel  
Chemistry Department  
Imperial College of Science  
Technology and Medicine  
London SW7 2AY (UK)  
Fax: (+44) 171-594-5804  
E-mail: d.goodgame@ic.ac.uk

[\*\*] This work was supported by the Engineering and Physical Sciences Research Council. The University of London Intercollegiate Research Service is thanked for the provision of facilities for solid-state NMR spectroscopy.

included catalytic unit (the “ship in a bottle” approach). The inclusion of features leading to chiral selectivity in catalytic processes also presents an extremely desirable, albeit challenging, goal.

There are, however, some serious problems that can vitiate the development of genuinely useful metal-organic zeotypes. These include, *inter alia*: a) the potential problem of organic matrix instability under the operating conditions that may be required for effective catalysis or separation process activity; b) the tendency of more flexible crystal lattices to “self-fill” any large potential “boxlike” cavities; c) the avoidance of the formation of such cavities by multiple three-dimensional (3D) lattice interpenetration.<sup>[3]</sup> Additionally, the cavities may be largely or completely occupied by counterions and/or solvent molecules, though the problem of solvent inclusion may not prevent zeotype usefulness if the solvent molecules can be removed without significant structural change leading to major loss of zeotype porosity. We report here an example of a novel, large-pore metal-organic zeotype which manages to circumvent, at least to a significant extent, most of these problems.

When equimolar amounts of zinc bromide and 2,4,6-tri(1-imidazolyl)-1,3,5-triazine (timt) were mixed in *N,N*-dimethylformamide (DMF) at room temperature a colorless crystalline solid was formed. X-ray structural examination<sup>[4]</sup> of the crystals obtained revealed that the reaction results in the conversion of timt to 4,6-di(1-imidazolyl)-1,3,5-triazine-2-one (Hdimto) (Scheme 1) which, in its deprotonated form, gives the complex  $[\text{Zn}(\text{dimto})_2]_n \cdot x(\text{DMF})$  (**1**). The same product was also formed when zinc bromide was replaced by zinc chloride or zinc iodide.



Scheme 1. Metal-catalyzed conversion of timt to dimto.

The anion of the 4,6-di(1-imidazolyl)-1,3,5-triazine-2-one molecule acts as a trinucleating ligand, binding to the metal ions through the two available imidazole nitrogen atoms and the carbonyl oxygen atom (Figure 1). These units self-assemble to form nearly planar tapes mutually inclined by 79° and joining at the zinc centers. Each dimto ligand is coplanar to within 0.19 Å, with the zinc atom bound to the oxygen atom lying within the plane, whilst those bonded to the nitrogen atoms lie 0.42 Å above and below the plane. The symmetry at each zinc center is  $D_2$ , the Zn–O and Zn–N distances being 2.116(5) and 2.138(5) Å, respectively; the angular departures from octahedral symmetry are less than 1°. An unusual feature of the ligand coordination is the Zn–O–C angle of 180°.<sup>[5]</sup>

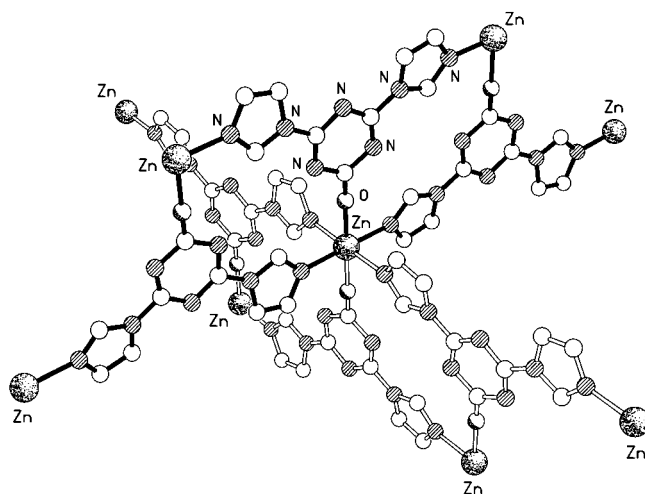


Figure 1. The coordination environment at one of the Zn centers in the solid-state structure of **1** showing the intersection of two approximately orthogonally oriented segments of the continuous tapes.

The motif illustrated in Figure 1 extends in three dimensions to form a set of contiguous boxlike units (Figure 2). The Zn···Zn separations around the equatorial belt of each box are 13.08 Å, the inter-Zn–Zn vector angles being 79/101° (see above). Each unit contains voids which interconnect to form

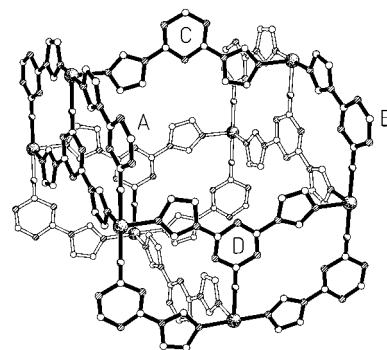


Figure 2. One of the boxlike units that extend to form the continuous three-dimensional network of **1**.

sinuous channels that extend in three dimensions. The windows into each of these channels are bounded by the ligands containing the triazine rings indicated A–D in Figure 2. Allowing for the van der Waals radii, the approximate window size is 9.6 × 5.5 Å. Figure 3 depicts a view of this porous structure viewed down the crystallographic 101 direction. A particularly important feature of this material is that, because of the uncharged nature of this array, there are no counterions to obstruct the pores.

Because of the very open nature of the  $[\text{Zn}(\text{dimto})_2]_n$  framework, at least some of the DMF molecules of solvation occluded in the lattice are lost on removal of the solid from solution and it is therefore difficult to obtain either a reproducible or a precise value for the DMF:Zn ratio from the X-ray study or from elemental analysis results. Thermogravimetric analysis measurements indicate a typical DMF:Zn ratio of about 6, and show that there is complete desolvation by about 170 °C. The desolvated lattice is then

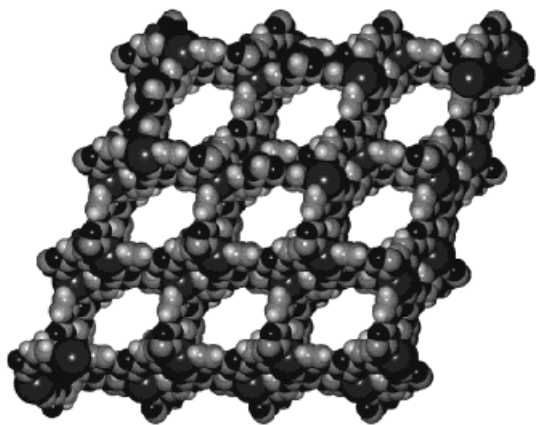


Figure 3. Space-filling representation of the solid-state structure of **1**, showing the large pores that extend through the structure.

thermally stable to about 300 °C after which gradual decomposition occurs. Desolvation can also be easily achieved at room temperature by immersing the solid in a more volatile small molecule solvent such as acetonitrile (which causes exchange of the included solvent molecules—see below), filtering off the solid, and then simply applying a vacuum to remove the occluded acetonitrile. X-ray powder patterns of the solvent-free matrix obtained by desolvation at room temperature show that there is no significant change in the structure. Even after direct thermal removal of the less volatile guests such as DMF (at about 140 °C) the gross lattice integrity appears to be retained.<sup>[6]</sup>

The sizes of the cavities and access channels in **1** offer appreciable potential for guest molecule uptake and this is under examination. The diamagnetism of the host  $[\text{Zn}(\text{dimto})_2]_n$  lattice permits the application of a particularly favorable way of studying the inclusion of guest molecules by means of solid-state magic angle spinning (MAS) NMR spectroscopy. This is illustrated in Figure 4 which shows the  $^{13}\text{C}$  MAS spectrum of the desolvated lattice and the analogous spectra of samples containing DMF or ethanol molecules, respectively.

The formation of this type of large-pore metal-organic zeotype is not restricted to zinc as the linking metal ion, as we have obtained, and structurally characterized, an analogous compound with manganese(II), thus demonstrating the feasibility of incorporating potentially redox-active metal centers into the lattice framework. This fact, when taken in conjunction with the size of the lattice cavities, the fundamental difference in the nature of the cavity “walls” as compared with the aluminosilicate zeolites, the absence of counterions, and a reasonable thermal stability, make these, and related, materials exciting new candidates for examination of their potential utility in, for example, catalysis or separation processes.

#### Experimental Section

Large colorless crystals of **1** formed over a two-day period from a solution containing zinc bromide (45 mg, 0.2 mmol) and 2,4,6-tri(1-imidazolyl)-1,3,5-triazine (56 mg, 0.2 mmol) in DMF (4 mL). Yield 70 % (based on  $\text{Zn}^{2+}$ ). Once separated from the mother liquor the crystals were sensitive to partial loss of the included DMF of solvation. The solid-state CP/MAS

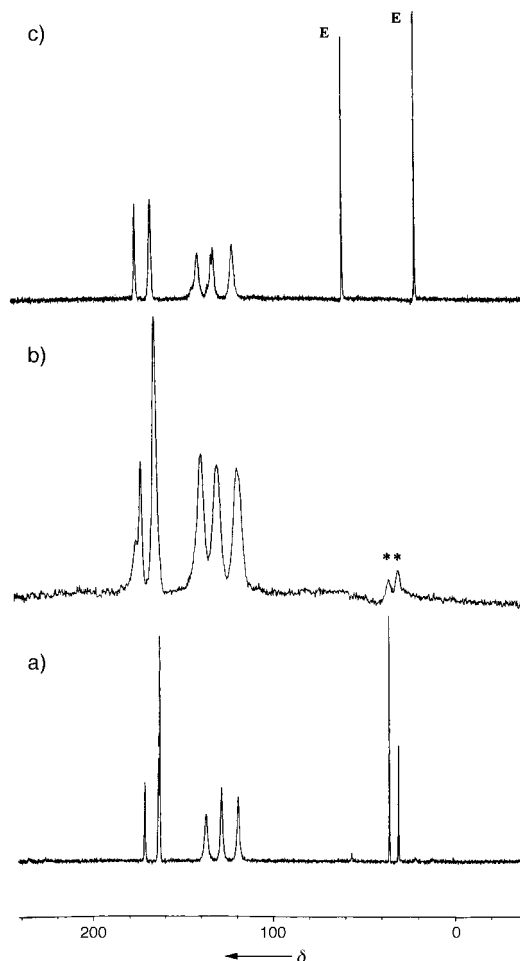


Figure 4.  $^{13}\text{C}$  MAS NMR spectra of a) compound **1**, peaks at  $\delta = 30.57$ ,  $35.49$ , and  $163.25$  are due to the  $^{13}\text{C}$  NMR resonances of DMF; b) compound **1** after almost complete removal of the included DMF (the peaks marked \* are due to small residual amounts of DMF); c) a sample of **1** in which the DMF has been replaced by ethanol (the  $^{13}\text{C}$  NMR resonances of ethanol are marked E).

$^{13}\text{C}$  NMR spectra were recorded at 75.5 MHz (7.05 T) on a Bruker MSL300 spectrometer and a standard Bruker magic angle sample spinning (MAS) probe with double-bearing rotation mechanism. The samples were studied at ambient probe temperature as polycrystalline powders in zirconia rotors (7 mm external diameter) and MAS frequencies between 4 and 5 kHz (with stability better than about  $\pm 10$  Hz) were used. The  $^{13}\text{C}$  chemical shifts are given relative to tetramethylsilane.

Received: July 20, 1998 [Z12178IE]  
German version: *Angew. Chem.* **1999**, *111*, 217–219

**Keywords:** microporosity • solid-state structures • supramolecular chemistry • zeolite analogues • zinc

- [1] I. W. C. E. Arends, R. A. Sheldon, M. Wallau, U. Schuchardt, *Angew. Chem.* **1997**, *109*, 1190–1211; *Angew. Chem. Int. Ed. Engl.* **1997**, *36*, 1144–1163.
- [2] a) C. Janiak, *Angew. Chem.* **1997**, *109*, 1499–1502; *Angew. Chem. Int. Ed. Engl.* **1997**, *36*, 1431–1434, and references therein; b) Subsequent to the submission of this communication, Yaghi and co-workers reported a microporous framework comprising zinc centers bonded to 1,4-benzenedicarboxylate anions, H. Li, M. Eddaoudi, T. L. Groy, O. M. Yaghi, *J. Am. Chem. Soc.* **1998**, *120*, 8571–8572.

- [3] For a recent comprehensive review of lattice interpenetration see: S. R. Batten, R. Robson, *Angew. Chem.* **1998**, *110*, 1558–1595; *Angew. Chem. Int. Ed.* **1998**, *37*, 1460–1494.
- [4] Crystal data for **1**:  $C_{18}H_{12}N_{14}O_2Zn_6C_3H_7NO$ ,  $M_r = 960.36$ , clear octahedron,  $0.30 \times 0.23 \times 0.20$  mm, orthorhombic, space group *Fddd*,  $a = 16.638(5)$ ,  $b = 20.198(3)$ ,  $c = 26.273(3)$  Å<sup>3</sup>,  $V = 8829(3)$  Å<sup>3</sup>,  $Z = 8$ ,  $\rho_{\text{calc}} = 1.445$  g cm<sup>-3</sup>,  $\mu(\text{CuK}\alpha) = 1.400$  mm<sup>-1</sup>,  $F(000) = 4032$ . Siemens P4 diffractometer, graphite-monochromated  $\text{CuK}\alpha$  radiation,  $\omega$  scans,  $T = 293$  K. Of 1650 independent reflections measured ( $2\theta < 120^\circ$ ), 1156 had  $I_0 > 2\sigma(I_0)$  and were considered observed. The structure was solved by direct methods and the non-hydrogen atoms were refined anisotropically. The hydrogen atoms were placed in calculated positions, assigned isotropic thermal parameters  $U(\text{H}) = 1.2U_{\text{eq}}(\text{C})$  and allowed to ride on their parent carbon atoms. Refinement was by full-matrix least-squares based on  $F^2$  to give  $R_1 = 0.0767$ , and  $wR_2 = 0.2143$ . Computations were carried out with the SHELXTL 5.03 program package. The included DMF solvent was distributed randomly throughout the channels in the structure and no realistic atom positions could be fitted to the weak diffuse areas of residual electron density. The value of about six DMF molecules per zinc atom given in the empirical formula was deduced from the TGA measurements and the corresponding values of calculated density,  $\mu$ , and  $F(000)$  reflect this figure. Crystallographic data (excluding structure factors) for the structures reported in this paper have been deposited with the Cambridge Crystallographic Data Centre as supplementary publication no. CCDC-102315. Copies of the data can be obtained free of charge on application to CCDC, 12 Union Road, Cambridge CB21EZ, UK (fax: (+44) 1223-336-033; e-mail: deposit@ccdc.cam.ac.uk).
- [5] A search of the April 1998 release of the Cambridge Crystallographic Database revealed only three other examples of a linear M-O-C arrangement out of a total of 1787 hits.
- [6] A substantial portion of the powder pattern of the heated sample comprises an amorphous “hump” but with the principal lines of the host structure clearly visible.

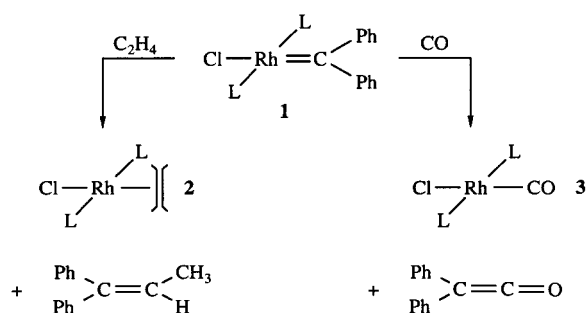
## The First Example of Linkage-Isomeric Ketene Metal Complexes\*\*

Elke Bleuel, Matthias Laubender,  
Birgit Weberndörfer, and Helmut Werner\*

*Dedicated to Professor Otto J. Scherer  
on the occasion of his 65th birthday*

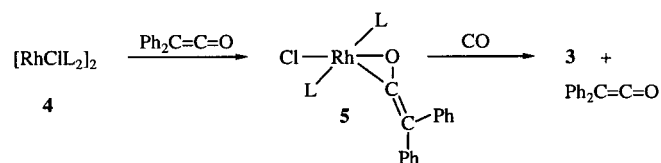
In the course of investigations on the reactivity of carbenerhodium complexes *trans*-[RhCl(=CR')(L)<sub>2</sub>] (R' = aryl; L = PR<sub>3</sub>, AsR<sub>3</sub>, SbR<sub>3</sub>) we recently observed<sup>[1]</sup> that these compounds react smoothly with olefins, CO, and isocyanides by C–C coupling. While the reaction of **1** with ethene affords **2** exclusively 1,1-diphenylpropene (and *not* 1,1-diphenylcyclopropane), treatment of **1** with CO forms the carbonyl complex **3** and diphenylketene (Scheme 1).<sup>[1, 2]</sup>

Since it is known from the work by the groups of Herrmann, Cutler, Roper, and others that reactions of both metal carbonyls with diazoalkanes and of metal carbenes with CO under pressure lead to ketene complexes,<sup>[3]</sup> we were inter-



Scheme 1. L = PiPr<sub>3</sub>.

ested to find out whether the metal-assisted formation of Ph<sub>2</sub>C=C=O from **1** and CO occurs via the intermediate *trans*-[RhCl(Ph<sub>2</sub>C=C=O)(PiPr<sub>3</sub>)<sub>2</sub>]. Attempts to detect such a compound by controlled addition of CO to a solution of **1** in C<sub>6</sub>D<sub>6</sub> or CDCl<sub>3</sub> failed. Therefore we chose a different synthetic route for our target, the square-planar ketenerhodium complex, and treated the chloro-bridged binuclear compound **4**<sup>[4]</sup> with diphenylketene. In benzene at room temperature complex **5** (Scheme 2) is readily formed and, after removal of the



Scheme 2. L = PiPr<sub>3</sub>.

solvent, is isolated as a red-brown solid in almost quantitative yield. The coordination of diphenylketene through the C=O and not the C=C bond, which was already indicated by the spectroscopic data,<sup>[3c]</sup> was confirmed by an X-ray crystal structure analysis (Figure 1).<sup>[5]</sup> The coordination geometry around the rhodium atom is distorted square-planar, the bond angle P1-Rh-P2 of 168.41(4)° thereby deviates considerably from the ideal value of 180°. We assume that this is due to the repulsion between the isopropyl and phenyl groups. Moreover, a remarkable feature is that in contrast to Cl-Rh-Cl (146.32(1)°) the axis Cl-Rh-O (177.25(9)°) is nearly linear and thus unsymmetrical bonding of the C=O unit to the metal center results. Compared to other  $\eta^2(\text{C}, \text{O})$ -diphenylketene complexes,<sup>[6]</sup> the distance O–Cl in **5** is significantly shorter which points to a reduced degree of  $\pi$ -back bonding from the rhodium center to the  $\pi^*$  orbital of the C=O moiety. In view of the presence of the electron-rich [RhCl(PiPr<sub>3</sub>)<sub>2</sub>] fragment this observation is really surprising.

The ketene complex **5**, which is thermally remarkably stable, reacts with CO under normal pressure to yield quantitatively the rhodium carbonyl compound *trans*-[RhCl(CO)(PiPr<sub>3</sub>)<sub>2</sub>]<sup>[7]</sup> and diphenylketene. Upon treatment of **5** with C<sub>6</sub>H<sub>7</sub>K in THF a substitution of chloride for indenyl does not occur. However, the desired ligand exchange can be carried out if compound **5** is transformed in the initial step with one equivalent of AgPF<sub>6</sub> to an intermediate with the supposed composition *trans*-[Rh(Ph<sub>2</sub>C=C=O)(PiPr<sub>3</sub>)<sub>2</sub>-(O=CMe<sub>2</sub>)]PF<sub>6</sub>, which subsequently reacts in situ with

[\*] Prof. Dr. H. Werner, Dipl.-Chem. E. Bleuel,  
Dipl.-Chem. M. Laubender, Dipl.-Chem. B. Weberndörfer  
Institut für Anorganische Chemie der Universität  
Am Hubland, D-97074 Würzburg (Germany)  
Fax: (+49) 931-888-4605  
E-mail: helmut.werner@mail.uni-wuerzburg.de

[\*\*] This work was supported by the Deutsche Forschungsgemeinschaft (SFB 347), the Fonds der Chemischen Industrie, and the BASF AG.